Stress distribution analysis of single overlap adhesive bonded joints - An analytical and numerical study

Brandão, Vinícius D.[1], Rodríguez, René Q.[1]

[1]Dept. of Mechanical Engineering, Federal University of Santa Maria
Avenida Roraima, 1000, 97105-900, Santa Maria/RS, Brazil
vinicius.brandao@acad.ufsm.br, rene.rodriguez@ufsm.br

Abstract. The present work aims to present a comparative study of stress distribution along a single lap bonded joint between analytical and numerical methods, which will be both 2D and 3D for further comparison. Through this comparison, it is expected to display the stress concentration behavior predicted in traditional solid mechanics bibliography, highlighting jap edges as main stress concentration areas as well as critical fracture regions, where the adhesive layer is likely to peel. For this analysis, a number of hypotheses are raised, such as an isotropic adherend (composed of steel), a homogenous adhesive lap joint and both adherend and adhesive components behave as elastic materials. The present study is based on the international standard ASTM D1002 [1] tensile test. This standard test is considered simple, especially given the low number of elements involved: two steel adherends and an adhesive lap joint. However, the test provides important information regarding the parameters that directly influence the stress distribution. The analytical methods used were modeled in the MATLAB® software, whereas the numerical methods were conceived in ABAQUS® finite elements software.

Keywords: Adhesive, Single lap joint; FEM analysis, Bonded joints, analytical methods, adhesive simulation

1 Introduction

The adhesively bonded joint is a modern technology that has seen increased demand in recent years. According to [2], the structural adhesives market grew to approximately U$18.3 billion in 2016, with a compound annual growth rate (CAGR) of approximately 7.9% from 2016 to 2022. The reason behind this expansion, according to the above-mentioned source, is due to the benefits found in using this technique for the bonding of joints. Among these we can mention high demand of lightweight materials for automotive, aeronautical, transportation, building and construction and furniture markets, good acoustic isolation, desirable rust prevention, homogeneous adhesive distribution, providing equivalent stress distribution and no alteration in metal properties due to heating. This paper reviews several linear and non-linear analytical models of stress distributions in adhesively bonded joints. For the calculation of the analytical methods, individual programs were coded for use in Matlab™ commercial software, which receives the part geometry, considering a single lap joint, including thickness of the adhesive layer, length and width, load applied and material property. In this regard, the Adhesive selected for analysis, and which parameters were used, was the ARALDITE AV138/HV998. Separate software is used to run all the analytical methods at once and generate a graphic displaying the results for each model. Similarly, the numerical method is modeled in Abaqus™, for subsequent part information input, assembly, step, boundary conditions, mesh and finally simulation execution. Finally, paths are created in key areas of the geometry to obtain stress distributions along longitudinal lines in the mesh along the width of the lap joint. These results are exported to Matlab as well, so that they can be displayed along with the analytical results. The failure criteria are established for each method, in order to define the strength for each analytical method, which can be compared to numerical data given by both 2D and 3D subsequent analyses. This way, a brief description of the criteria is provided. According to Clifford [13], the criteria used for this static analysis case is the maximum shear stress concept. The geometric model, with dimensions in mm, is shown in Figure 1.

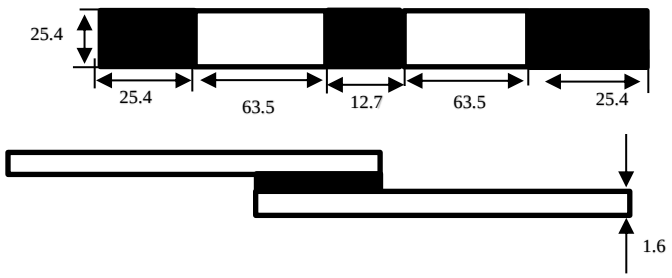

[mm]

Figure 1. Chosen geometry

Analytical Methods

In this section, the analytical methods will be presented in detail, in order to clarify the mathematical procedure. These equations differ from each other, for as time progressed, the models proposed by early authors were further developed, enriched, and new aspects were included in the analysis.

2.1 Volkersen Model

The pioneering work by Volkersen [3] is the first known method in the literature for the analysis of stress distribution in bonded joints. This method is also known as the shear-lag model, introduced the concept of differential shear, however it did not take into account the eccentricity of the load path inherent of this geometry. The adhesive shear stress distribution is given by:

$$\tau = \frac{P.\omega}{2.b}.\frac{cos\,(\omega x)}{sinh\left(\frac{\omega t}{2}\right)} + \left(\frac{t_t - t_b}{t_t + t_b}\right).\left(\frac{\omega l}{2}\right).\frac{sinh\,(\omega x)}{cosh\left(\frac{\omega l}{2}\right)}, \tag{1}$$

where:

$$\omega = \sqrt{\frac{G_a}{E t_t t_a}.\left(1 + \frac{t_t}{t_b}\right)}.$$

In this equation, *w* is the shear-lag distance, the velocity in which the load is transferred from one adherend to the other, t_t is the upper adherend thickness (steel plate), consequently t_b is the bottom adherend thickness and t_a is the adhesive layer thickness. Additionally, *b* is the bonded area thickness, for a given l length, *P* is the force applied in the simulation, G_a is the adhesive shear modulus and E is the adherend elasticity modulus. The center of the overlap is placed at the origin of the system, which is taken into account when replacing *x* values. With the desire to keep the design adhesive stresses to a minimum, both the adherends are rendered equal in thickness, as well as, according to Rodríguez [14], it is assumed that the joint is sufficiently long such that sinh(*wl*) = cosh(*wl*), which gives the simplified equation:

$$\tau = \frac{\omega P}{2} = \sqrt{\frac{G_a}{E t_t t_a}.\left(1 + \frac{t_t}{t_b}\right).\frac{P}{2}}. \tag{2}$$

Analyzing this formula, it is assumed that the magnitude of the peak adhesive stress is independent of the joint length for long joints, increases with increasing adhesive shear modulus and also with decreasing adherend modulus and thickness, plus adhesive thickness.

2.2 Goland and Reissner

A further development upon the Volkersen [3] model, the Goland & Reissner [4] one built upon the previous work by introducing bending effects due to eccentric load in the mathematical model. For this end, the problem was composed of analyzing the bending of the adherend away from the lap region with length l and area a. Then, the region of the lap joint is analyzed, with length 2*c* and thickness *t*. Similar to the previous equations, the shear stress distribution is given by:

$$\tau = -\frac{1}{8}\frac{\bar{P}}{c}.\left\{\frac{\beta c}{t}(1+3k)\frac{cosh\left(\frac{\beta c x}{t\ c}\right)}{sinh\left(\frac{\beta c}{t}\right)}+3(1-k)\right\}, \tag{3}$$

where $\bar{P}$ is the applied tensile load per unit width, *c* is half the overlap length, t is the adherend thickness, α is Poisson's ratio and k is the bending factor:

$$k = \frac{cosh\,(u_2 c)}{cosh(u_2 c)+2\sqrt{2}sinh\,(u_2 c)}, u_2 = \sqrt{\frac{3(1-\alpha^2)}{2}}\frac{1}{t}\sqrt{\frac{\bar{P}}{tE}},\ \beta^2 = 8\frac{G_a}{E}\frac{t}{t_a}.$$

The adhesive peel stress distribution is given by:

$$\sigma = \frac{1}{\Delta}\frac{\bar{P}t}{c^2}[A+B], \tag{4}$$

where:
$A = (R_2\delta^2\frac{k}{2}+\delta k'\,cosh(\delta)\,cos(\delta)\,)cosh\left(\frac{\delta x}{c}\right)cos\left(\frac{\delta x}{c}\right), B = (R_1\delta^2\frac{k}{2}+k'\,sinh(\delta)\,sin(\delta)\,)sinh\left(\frac{\delta x}{c}\right)sin\left(\frac{\delta x}{c}\right).$

And $k' = \frac{kc}{t}\sqrt{3(1-\alpha^2)\frac{\bar{P}}{tE}}$ is the transverse force factor. Additionally:

$$\delta = \gamma\frac{c}{t}, \gamma^4 = 6\frac{E_a}{E}\frac{t}{t_a}, \Delta = \frac{1}{2}(sin(2\delta)+sinh(2\delta)).$$

Also:

$$R_1 = cosh(\delta)\,sinh(\delta)+sinh(\delta)\,cos(\delta)\,, R_2 = -cosh(\delta)\,sin(\delta)+sinh(\delta)\,cos\,(\delta).$$

2.3 Hart-Smith

In a report for NASA, Hart-Smith [5] considered adhesive plasticity for single lap joints combining elastic peel stress with plastic shear stresses, where the distribution is given by:

$$\tau(x) = A_2\,cosh(2\delta' x)+C_2, \tag{5}$$

where:

$$\delta' = \sqrt{\left[\frac{1+(3-\alpha^2)}{4}\right]\frac{2G_a}{t_a E t}},\ A_2 = \frac{G_a}{t_a E t}\left[\bar{P}\frac{6(1-\alpha^2)M}{t}\right]\frac{1}{2\delta'\,sinh(2\delta' c)},\qquad C_2 = \frac{1}{2c}\left[\bar{P}-\frac{A_2}{\delta'}sinh(2\delta' c)\right],$$

$$M = \bar{P}\left(\frac{t+t_a}{2}\right)\frac{1}{1+\varepsilon\beth+\left(\frac{\beth^2 c^2}{6}\right)}, \beth^2 = \frac{\bar{P}}{D'}, \tag{6}$$

and $D = \frac{Et^3}{12(1-\alpha^2)}$ is the adherend bending stiffness. Variables $\bar{P}$, *Ga*, *ta*, *E*, *Ea*, α , *t*, *c* has the same meaning as presented by Volkersen and Goland & Reissner models. The adhesive peel stress distribution σ(x) is given by:

$$\sigma(x) = Acosh(\times x)\,cos(\times x)+Bsinh(\times x)sin\,(\times x). \tag{7}$$

Additionally, there is a plastic stress model using bi-linear elastic-perfectly plastic approximation. The adhesive lap is divided into three regions, whereas the center one is elastic with length d and two plastic ones with length $\frac{l-d}{2}$. The coordinates *x* and *x'* are defined in Figure 2.

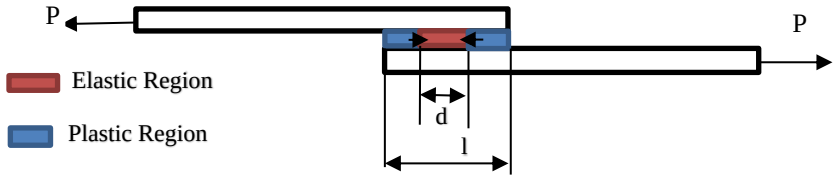

Figure 2. Elastic and plastic interface proposed by Hart-Smith

The solution to the problem in the elastic region is given by the shear stress:

$$\tau(x) = A_2\, cosh(2\delta' x) + \tau_p(1-K). \tag{8}$$

The shear strain for the plastic region is:

$$2\left(\frac{\gamma_p}{\gamma_e}\right) = K\{\left[2\delta'\left(\frac{l-d}{2}\right)\right]^2 + tanh(\delta' d)\}, \tag{9}$$

where γ_e and γ_p are the shear strain for the elastic and plastic regions, respectively.

2.4 Ojalvo & Eidinoff

Ojalvo & Eidinoff [6] model is built upon the Goland & Reissner [4] model, with modified coefficients in the shear stress equations, adding new terms for the differential equation along with new boundary conditions for bond peel stress calculation. In the scope of their work, they proposed a model that expresses the variation of shear stress along the bond layer thickness, which was a new approach to the problem. As procedure, the adhesive non-dimensional stress distribution for this model is given by:

$$\tau^* = Acosh\left(\delta\sqrt{2+6(1+\beta)^2 x^*}\right) + B, \tag{10}$$

where:

$$A = \frac{2\delta(1+3(1+\beta)^2 k)}{\sqrt{2+6(1+\beta)^2}\, sinh\left(\delta\sqrt{2+6(1+\beta)^{2x^*}}\right)}, B = 1 - \frac{Asinh\left(\delta\sqrt{2+6(1+\beta)^2}\right)}{\delta\sqrt{2+6(1+\beta)^2}},$$

$$\delta^2 = \frac{G_a c^2}{E^* th} \; and \; \beta = \frac{h}{t}.$$

Considering $E^* = E$ for adherends in plane stress and $\frac{E}{1-\alpha^2}$ for adherends in plane strain. Repeated variables from previous models represent the same as previously, plus h is the adhesive thickness, k is the bending moment factor similar to the one present in the Hart-Smith [5] model. The maximum non-dimensional stress observed at the interfaces is given by:

$$\tau^{**} = \tau^* \pm \Delta\tau^*. \tag{11}$$

where:

$$\Delta\tau^* = \frac{G_a h}{2E_a}\sigma^{*\prime}. \tag{12}$$

The solution for the nondimensional peel stress (σ^*) is given by:

$$\sigma^* = Csinh(\alpha_1 x^*)\, sin(\alpha_2 x^*) + Dcosh(\alpha_1 x^*)\, cos(\alpha_2 x^*), \tag{13}$$

where:

$$\alpha_1^2 = \frac{3\beta\delta^2}{2} + \frac{\rho}{2};\ \alpha_2^2 = -\frac{3\beta\delta^2}{2} + \frac{\rho}{2}\ and\ \rho^2 = \frac{24E_a c^4}{E^* h t^3}.$$

Considering that the constants D and C are acquired from the substitution of the derivatives of (14) into (15) and (16):

$$\sigma^{*\prime\prime}(\pm 1) - 6\beta\gamma^2\sigma^{*\prime}(\pm 1) = \mp k\gamma\rho^2(1+\beta),\ \sigma^{*\prime\prime}(\pm 1) = k\gamma\rho^2(1+\beta), \tag{14}$$

where $\gamma = \frac{t}{2c}$.

3 Numerical methods

In this section is presented the numerical validation of the problem solution, utilizing the commercial software ABAQUS®, including geometry, property, mesh specifics and boundary conditions. The results from this process are used to compare to the analytical data. As boundary conditions, the sample was fixed at one end in the adherend and pulled by the other end of the second adherend, which creates a tensile test with eccentric loading of 5000N. The mesh generated for the study was tridimensional, of the type C3D8R, an 8-node reduced integration linear quadrilateral element of the 3D stress family for the 3D model. The total number of elements is 1300 linear hexahedral of the C3D8R type, with 3090 nodes connecting them. Since the object was modelled in 3D, the stress distribution across the part transversally is composed of several different paths, which are further investigated in this study. After the simulation was completed, each path created by the mesh was selected for plotting the stress distribution and including these results into the final analysis. The paths created for analysis are shown in Figure 3:

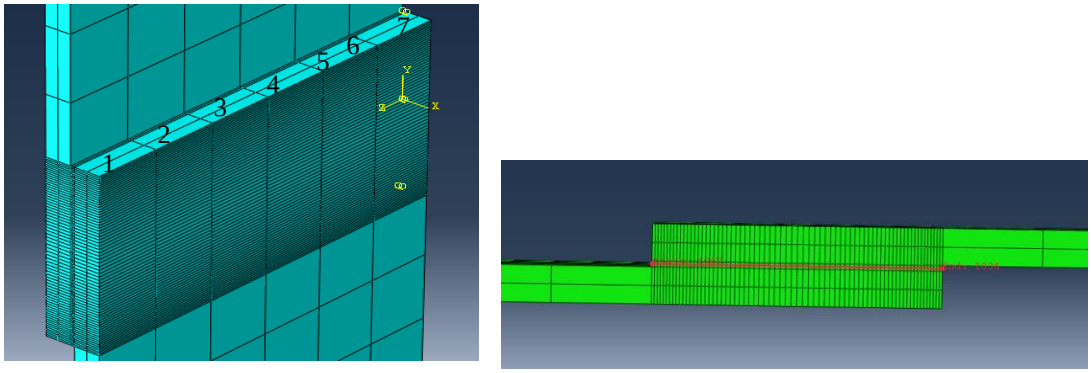

(a) (b)

Figure 3. 3D and 2D FEM geometries (including paths).

Additionally, the stress contour plot in the geometry's simulation, for both shear and peel stresses, is shown in Figure 4.

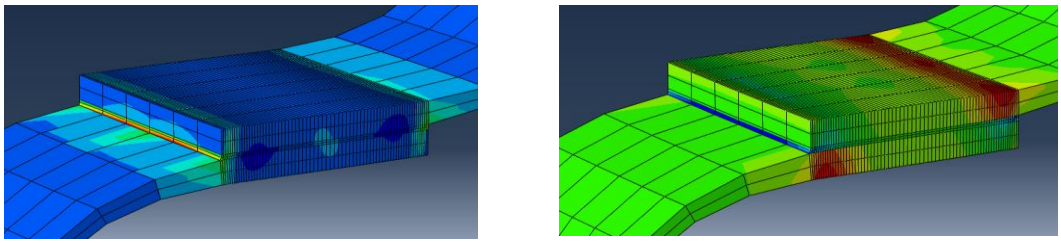

(a) (b)

Figure 4. Shear (a) and Peel (b) stress distributions in contour, displaying the tridimensional simulation

4 Results

In the following section, all the results obtained from experimental studies are displayed and compared, so that they can be analyzed in the conclusions section. The stress distribution for shear and peel given by the FEM software in a contour style have both been displayed, so as to provide a reference of the regions where the stresses are concentrated and most heavily affect the adhesive layer's resistance. Additionally, the stress distribution is investigated using multiple paths across the width of the geometry, in order to present a deeper inspection of this property. Therefore, after presenting the corresponding analytical and numerical models considered, the graphical comparison between models is given in Figure 5, considering the edge paths and middle of the thickness paths respectively.

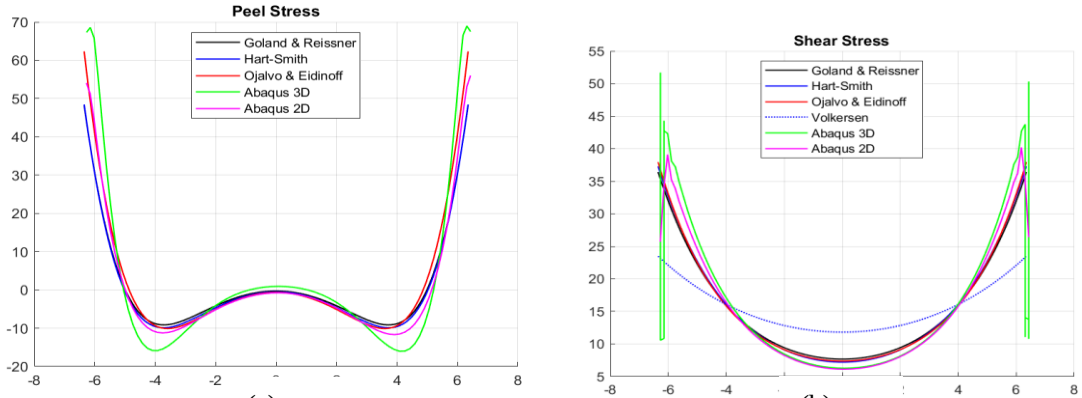

(a) (b)

Figure 5. (a) Shear and (b) Peel stress distributions for all the models considered and an edge path (1) for the 3D model

These images show the stress distribution compared to two of the total 7 paths of analysis. This choice was made in order to represent two opposite circumstances, one of the paths is in the geometry edge and the other is in the middle. However, all of the paths have been computed and the maximum stresses for peel and shear have been compelled in a table to more appropriately arrange this information.

Table 1. Maximum stresses for each model

Models/Maximum Stress	Peel (MPa)	Shear (MPa)
3D FEM path 1	46.26	39.44
3D FEM path 2	60.43	51.69
3D FEM path 3	68.93	51.69
3D FEM path 4	62.92	49.45
3D FEM path 5	68.95	51.52
3D FEM path 6	60.07	51.52

3D FEM path 7	45.49	39.31
2D FEM	56.01	40.19
Volkersen	-	23.48
Goland & Reissner	48.24	36.4
Hart-Smith	48.45	37.28
Ojalvo & Eidinoff	62.31	37.94

The results give a good notion of the safety factor included in each method, considering the failure criteria presented previously. All the models but Goland & Reissner [4] used a shear stress failure criteria, given that it represents the critical stress value for the joint.

5 Conclusions

The adhesive overlap joint study is a fairly new concept to mechanical designs, hence there are several models that aim to predict as best as possible the behavior of the adherends and adhesives in such an application, especially given the parameters which vary from one joint to another, whether it is a joint method difference or just the dimensions of the parts joint together or the adhesive. The results presented show that the more modern analytical models of determining the stress distribution are fairly accurate compared to older ones, which undoubtedly should be confirmed with adhesive thickness variation or plastic behavior included. As such, the 3D FEM method show quite apparent differences in the maximum and minimum stress curves for both peel and shear distributions, compared to both 2D and analytical models. This evidence provides a further understanding of how the analytical analysis can improve and might indicate areas of improvement in structural projects that made use of some of the models presented. The 3D FEM analysis is important because it allows for further developments on overlap joint bonding taking into account the uneven distribution of stress through the adhesive layer's thickness.

References

[1] ASTMD1002, 2001. Standard Test Method for Apparent Shear Strength of Single-Lap-Joint Adhesively Bonded Metal Specimens by Tension Loading (Metal-to-Metal).
[2] Market Research Future. Structural Adhesives Market. Available at https://www.marketresearchfuture.com/reports/structural-adhesives-market-2177. Accessed in 22/7/2021.
[3] Volkersen, O., 1938. "Nietkraftverteiligung in zugbeanspruchten nietverbindungen mit konstanten laschenquerschnitten". Luftfahrtforschung, Vol. I, pp. 15–41.
[4] Goland, M. and Reissner, E., 1944. "The stresses in cemented joints". Journal of Applied Mechanics, Vol. 11, pp. A17–A27.
[5] Hart-Smith, L.J., 1973. "Adhesive-bonded single-lap joints". Technical report, NASA CR-112236.
[6] Ojalvo, I. and Eidinoff, H., 1978. "Bond thickness effects upon stresses in single-lap adhesive joints". American Institute of Aeronautics and Astronautics Journal, Vol. 16, No. 3, pp. 204–211.
[7] Harris, J. and Adams, R., 1984. "Strength prediction of bonded single lap joints by non-linear finite element methods". International Journal of Adhesion and Adhesives, Vol. 4, No. 2, pp. 65–78.
[8] Hart-Smith, L.J., 1983. "Designing to minimize peel stresses in adhesive-bonded joints". In Delamination and Debonding of Materials. Pittsburgh, Pennsylvania, USA, pp. 238–266.
[9] Greenwood, L., Boag, T. and McLaren, A., 1969. "Stress distribution in lap joints". In Adhesion: Fundamentals and practice. pp. 273–279.
[10] Ikegami, K., Takeshita, T., Matsuo, K. and Sugibayashi, T., 1989. "Strength of adhesively bonded scarf joints between glass fibre reinforced plastics and metals". In Proceeding of Structural Adhesives in Engineering II.
[11] Charalambides, M., Kinloch, A. and Matthews, F., 1997. "Strength prediction of bonded joints". In AGARD Conference on Bolted/ Bonded Joints in Polymeric Composites. AGARD Conference Proceedings CP-590.
[12] da Silva LFM, Rodrigues T, Figueiredo M, Moura MD, Chousal J. Effect of adhesive type and thickness on the lap shear strength. J Adhes 2006;82(11):1091–115.
[13] Stein N, Weißgraeber P, Becker W. A model for brittle failure in adhesive lap joints of arbitrary joint configuration. Composite Structures 2015;133:707-718.
[14] Rodríguez R, Paiva W, Sollero P, Rodrigues M, Albuquerque E. Failure criteria for adhesively bonded joints. International Journal of Adhesion & Adhesives 2012;37:26-36.

Authorship statement. The authors hereby confirm that they are the sole liable persons responsible for the authorship of this work, and that all material that has been herein included as part of the present paper is either the property (and authorship) of the authors, or has the permission of the owners to be included here.